PCCP

Accepted Manuscript

ROYAL SOCIETY OF CHEMISTRY

www.rsc.org/pccp

Dissecting the steps of CO_2 reduction: 2. The interaction of CO and CO_2 with Pd/γ-Al_2O_3: *an in situ FTIR study*

János Szanyi*, Ja Hun Kwak[#]

Institute for Integrated Catalysis, Pacific Northwest National Laboratory

Richland, WA 99352

E-mail: janos.szanyi@pnnl.gov

[#]Current address: Department of Chemical Engineering, UNIST
100 Banyeon-Ri, Ulsan 689-798, Korea

TOC:

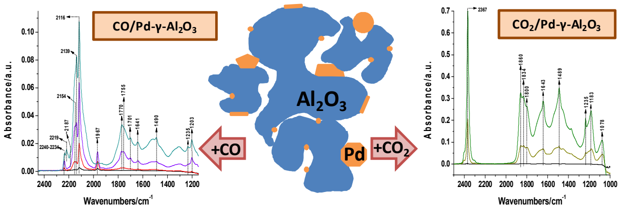

Surface species formed on Pd/γ-Al_2O_3 upon CO_x exposure will aid mechanistic studies of CO_2 reduction.

Dissecting the steps of CO_2 reduction: 2. The interaction of CO and CO_2 with Pd/γ-Al_2O_3: *an in situ FTIR study*

János Szanyi*, Ja Hun Kwak[#]

Institute for Integrated Catalysis, Pacific Northwest National Laboratory

Richland, WA 99352

E-mail: janos.szanyi@pnnl.gov

[#]Current address: Department of Chemical Engineering, UNIST
100 Banyeon-Ri, Ulsan 689-798, Korea

Abstract

Alumina supported Pd catalysts with metal loadings of 0.5, 2.5 and 10 wt% were investigated by in situ FTIR spectroscopy in order to understand the nature of adsorbed species formed during their exposure to CO_2 and CO. Exposing the annealed samples to CO_2 at 295 K resulted in the formation of alumina support-bound surface species only: linear adsorbed CO_2, bidentate carbonates and bicarbonates. Room temperature exposure of all three samples to CO produced IR features characteristic of both ionic and metallic Pd, as well as bands we observed upon CO_2 adsorption (alumina support-bound species). Low temperature (100 K) adsorption of CO on the three samples provided information about the state of Pd after oxidation and reduction. Oxidized samples contained exclusively ionic Pd, while mostly metallic Pd was present in the reduced samples. Subsequent annealing of the CO-saturated samples revealed the facile (low temperature) reduction of PdO_x species by adsorbed CO. This process was evidenced by the variations in IR bands characteristic of ionic and metallic Pd-bound CO, as well as by the appearance of IR bands associated with CO_2 adsorption as a function of annealing temperature. Samples containing oxidized Pd species (oxidized, annealed or reduced) always produced CO_2 upon their exposure to CO, while CO_2-related surface entities were observed on samples having only fully reduced (metallic) Pd.

Introduction: The reduction of CO_2 on oxide-supported metal catalysts requires the activation of both CO_2 and H_2 [1]. The interaction of CO_2 with metals is rather weak, and the formation of adsorbed species with appreciable life time on the metal surface takes place only in the presence of dopants (e.g., alkali dopants on Pt-group metals aid the formation of carbonites) [2-8]. On the other hand, metal particles are required to activate (i.e., dissociate) H_2 molecules. In our recent study on the reduction of CO_2 with H_2 on Pd/Al_2O_3 catalysts we have shown that the oxide support played a critical role in the activation of CO_2 [9]. The alumina not only ensured a high metal dispersion, but also actively participated in the reaction. When an inert multiwall carbon nanotube (MWCNT) replaced the alumina support no activity for the reduction of CO_2 was observed. However, when an oxide promoter was added to a Pd/MWCNT catalyst, its activity and product selectivity were very similar to that observed for the Pd/Al_2O_3 sample at comparable Pd loading. These results clearly indicated that CO_2 reduction requires bifunctional catalysts. In the first part of this study we examined the interaction of CO and CO_2 with the γ-Al_2O_3 support used throughout these studies, while here we report the results of our FTIR investigations on the adsorption of CO and CO_2 on Pd/γ-Al_2O_3 catalysts at Pd loadings of 0.5, 2.5 and 10 wt%.

The interaction of CO with Pd particles supported on a number of oxides has been studied extensively. The variation in the nature of the adsorbed species with metal particle size and support characteristics has been discussed in great details [10 and references therein]. In most cases, CO adsorbed on the low index crystal faces of metal particles was correlated with that on metal single crystals. Support materials strongly interacting (primarily oxides) with the metal particles were shown to significantly influence the adsorption properties of the metals by modifying their geometric and electronic structures. The interaction of CO_2 with supported metal catalysts has been investigated much less extensively, and it was shown that as a result of CO_2 adsorption/reaction over these systems carbonates and bicarbonates formed primarily on the oxide support. The role of these rather stable surface species in the conversion of CO_2 has been suggested in certain systems, while discounted in others [11].

Pure alumina as well as alumina with metal particles readily forms stable bicarbonates upon exposure to CO_2 under ambient conditions [12-14]. Furthermore, the formation of bicarbonates was also reported to take place on both pure and metal-loaded aluminas when they were exposed to CO only [13,14]. The formation of carbonates from CO only in these systems was explained by the participation of defect sites present on the surface of the alumina support. On the other hand, Magnacca and Morterra claimed that no bicarbonates could form on pure alumina in the absence of any metal [12].

The primary goal of this study was to identify and characterize the surface species formed in the Pd/Al_2O_3 systems upon their exposure to CO and CO_2. The results obtained in these studies will aid our ongoing *in situ* and *in operando* investigations on the reduction of CO_2 with H_2 on supported Pd catalysts.

Experimental: The γ-Al_2O_3 used throughout these studies was a commercial SBA-200 Puralox material from Condea with a BET surface area of 200 m^2/g. The supported 0.5, 2.5 and 10 wt% Pd/γ-Al_2O_3 catalysts were prepared by the incipient wetness method using $Pd(NH_3)_4(NO_3)_2$ as the precursor. The catalysts were activated in accordance to the activity measurements reported earlier [9].

The IR measurements were carried out on a Bruker Vertex 80 spectrometer equipped with a liquid nitrogen-cooled MCT detector, operated at 4 cm^{-1} resolution. Each spectrum reported was the average of 256 scans, and referenced to the spectrum of the clean sample. The IR cell is a modified 2 ¾" stainless steel cube equipped with KBr windows and connections to pumping stations and a gas handling system. The sample holder rod has ceramic feedthrough for heating and thermocouple connections. The powder samples (γ-Al_2O_3 support and Pd/γ-Al_2O_3 catalysts) were pressed onto a tungsten mesh which was attached to copper heating legs allowing resistive heating of the samples (temperature range: 100 – 1000 K). The temperature of the sample was monitored by a thermocouple spot welded to the top center of the tungsten mesh. The pressure in the IR cell could be controlled between 2×10^{-8} and 760 Torr. Oxygen and hydrogen gas used for cleaning and reduction of the samples were used as received (both gases were research purity). The CO and CO_2 used in the adsorption measurements were purified: CO was kept under liquid nitrogen in order to eliminate any metal-carbonyl impurities might be present in the metal cylinder-stored CO, while CO_2 was cleaned by cycles of freeze/pump/thaw. A typical experiment was conducted by first pre-treating the sample (annealing, oxidizing or reducing of the Pd/γ-Al_2O_3 catalysts) and then carrying out the adsorption experiments. The adsorbate (CO_2 or CO) was added to the cell in a desired amount and after equilibration an IR spectrum was collected. The stepwise addition of the adsorbate was continued until the equilibrium pressure in the IR cell was ~0.3 Torr. Then the cell was evacuated and the removal of adsorbed species was monitored by IR as a function of evacuation time. The adsorption of CO_2 was always carried out at 295 K, while the adsorption of CO was studied at both 100 and 295 K. The low temperature

CO adsorption was carried out to avoid the possible reduction of PdO_x species by CO at ambient temperature.

The electronic states of Pd particles in the different catalysts after oxidation and reduction treatments were monitored by in situ XPS. The three catalysts were loaded onto a sample holder carusel in an atmospheric pressure chamber attached to the XPS instrument, and the samples were treated under oxidizing or reducing gas flows at elevated temperatures. After the completion of the decomposition, oxidation and reduction steps the catalysts were transferred into the UHV compartment of the system for XPS analysis. (The results of these XPS measurements are summarized in panels ***a*** and ***b*** of Fig. S1 in the supplementary information for the oxidized and reduced samples, respectively.)

Results and Discussion: 1. CO_2 adsorption at 295 K: The interaction of CO_2 with the Pd/Al_2O_3 samples was investigated at 295 K sample temperature. Prior to CO_2 exposure the samples were calcined in O_2 flow at 773 K ex situ, mounted in to the IR cell and annealed at 773 K for 2 h under vacuum (P~2*x*10^{-8} Torr). The three series of IR spectra obtained from these annealed samples are displayed in Fig. 1 for 0.5 (a), 2.5 (b), and 10 wt% Pd/γ-Al_2O_3 (c) catalysts. The IR features observed for all three samples represent adsorbed species identical to the ones we had detected for the 773 K-annealed γ-Al_2O_3 support in the absence of any metal, i.e., adsorbed CO_2 (2340-2370 cm^{-1}), bridging carbonates (1060, 1410, 1700-1900 cm^{-1}) and bicarbonates (1235, 1485, 1645, 3610 cm^{-1}) [IR peak assignments were summarized in Table S1 in Part 1 of this study]. At room temperature no IR feature of CO_2 interacting with Pd particles were observed, consistent with prior findings that showed very weak interaction between Pt-group metals and CO_2 [2-8]. There is a dramatic decrease in intensity of the IR feature representing adsorbed CO_2 (2367 cm^{-1}) as the Pd coverage increases from 0.5 to 2.5 and finally to 10 wt%. This IR band has been assigned to CO_2 adsorbed onto surface defect site formed by the removal of hydroxyl groups from the alumina support [Part 1 of this study, and references therein]. The results presented in Fig. 1 suggest that Pd atoms/particles occupy these defect sites, thus efficiently blocking the sites for CO_2 adsorption. The quantitative correspondence between Pd loading and the number of defect sites is not possible from the data presented here, since the amounts of catalysts present in the three experiments are not identical. However, the qualitative trend is obvious: as the Pd coverage increases the number of surface defect sites where CO_2 can adsorb decreases. In our prior studies on γ-Al_2O_3 we have shown that pentacoordinate Al^{3+} (Al_p) ions formed by thermal treatment of γ-Al_2O_3 due to dehydroxylation, and this process starts just around 473 K, and it is completed by 673 K [15]. At low loading levels both metals (e.g., Pt) [16] and metal oxides (e.g., BaO and La_2O_3) [17] were shown to occupy pentacoordinate Al^{3+} sites on the (100) facets of the alumina particles in a 1:1 correspondence. After the saturation of these defect sites the formation of 2D rafts and 3D particles occur. Based on these results one may assume that Pd also binds to the same Al_p sites Pt and BaO. At this point, however, we do not have experimental evidence to support this assumption, but we can safely state from the results of this study that Pd binds to the alumina surface at Lewis acidic sites (sites created after the removal of surface hydroxyl groups). At the lowest Pd loading of this study (0.5 wt%) only a fraction of the surface Al^{3+} sites are occupied by Pd, and the intensity of the IR feature representing adsorbed CO_2 is the highest. When the Pd loading is increased to 2.5 wt% the intensity of this IR feature decreases by about 70 %. Furthermore, on the 10 wt% sample the intensity of the IR feature of the adsorbed CO_2 is very low (about 2 % of intensity of the 0.5 wt% Pd-loaded sample), as most of the defect sites on this sample are occupied by Pd. Note that the intensities of the IR features of bicarbonates (1235, 1485, 1645, 3610 cm^{-1}) vary with the Pd loading as well. In the IR spectra of the two low Pd-loaded samples these features exhibit similar intensities, while on the 10 wt% Pd-loaded catalyst the intensities of these IR features are very low. These observations support our conclusion that at low Pd loadings metal particles preferentially occupy Lewis acidic sites (i.e., surface Al^{3+} sites) and the hydroxyl groups still present after the 773 K annealing can react with CO_2 to form bicarbonates, and some weakly held bridging carbonates as well. On the other hand, at high Pd loadings the large metal particles occupy a large fraction of the surface and prevent the formation of bicarbonates (carbonates) on the alumina. Very similar IR intensities of adsorbed CO_2 and bicarbonates were observed on the annealed and reduced Pd/ γ-Al_2O_3 catalysts at low Pd loadings (data is not shown). However, on the 10 wt% Pd/γ-Al_2O_3 we observed an approximately three times increase in the intensity of the bicarbonate features after reduction in H_2 at 773 K, due, most probably, to the formation of large metal particles during the reduction process. As these large metal particles form more of the alumina surface becomes free and accessible for CO_2 adsorption.

2. CO adsorption at 295 K: The adsorption of CO on the three Pd/γ-Al_2O_3 catalysts was investigated at both 295 and 100 K sample temperatures. The low temperature study was carried out in order to minimize reaction between the catalyst and the adsorbate during CO adsorption. In order to identify adsorbed surface species on the 0.5, 2.5 and 10 wt% Pd/γ-Al_2O_3 catalysts, and the formation of carbonates and bicarbonates on the alumina support, CO adsorption experiments were conducted on all three catalyst samples after annealing at 773 K, oxidation at 573 K and reduction at 573 K. In our study of CO adsorption on the metal-free γ-Al_2O_3 support we observed no IR bands representing either adsorbed CO, CO_2 or carbonates/bicarbonates. This finding was in accord with the results of a prior investigation by Morterra and Magnacca [12], but contradicted the results reported by Föttinger and co-workers [14]. In this latter study the formation of carbonates/bicarbonates was observed on both the metal-free γ-Al_2O_3 support and on Pd/γ-Al_2O_3 catalysts upon CO exposure. Utilizing isotopically labeled CO and CO2 they explained the formation of carbonates by a “water gas shift reaction” mechanism on both pure alumina and Pd/γ-Al_2O_3. Their reaction mechanism involved and oxygen-down CO interacting with a surface defect and subsequently reacting with an adjacent surface hydroxyl group.

The electronic state of the Pd particles in the three samples studied in CO adsorption by IR spectroscopy was investigated by XPS. Although the conditions of reduction and oxidation treatments in the XPS experiments were somewhat different from those we could apply in the IR studies, the information we obtained are still relevant to these systems. Fig. S1 in the Supplementary Information displays two sets of XPS spectra in the Pd 3d binding energy (BE) region: for the oxidized (panel a) and for the reduced (panel b) samples. The binding energy values in the two sets of the spectra differ substantially indicating the presence of Pd species in different oxidation states after the two treatments: after oxidation the 3d binding energies of Pd particles are higher (by ~2 eV) in accordance with the presence of ionic species. The binding energy values in the reduced samples are much closer to each other in the three Pd-loaded samples. The binding energies for the three Pd-loaded samples after oxidation varies systematically: highest in the 0.5wt% Pd/γ-Al_2O_3 catalyst, and lowest in the 10 wt% sample. These differences can arise from the different particle sizes, the fundamentally different interactions of the Pd particles with the support (alumina) at different particles sizes, and the possible variation in the extent of oxidation. In the presence of large Pd clusters (10 wt%

sample) it is possible the not the entire metal particle was oxidized to Pd $^{2+}$ under the conditions applied, while in the 0.5 wt% sample (as all the Pd atoms are exposed) the oxidation was complete. The strong interaction between Pd atoms and the alumina surface may also result in the increased BE value at very high dispersion (0.5 wt% sample). Upon the reduction treatment applied most of the Pd was reduced to Pd^0, however, some Pd atoms are still present in the $\delta+$ oxidation state at low Pd loading. (this might be even more pronounced in our IR studies where the reduction conditions were significantly milder: lower H_2 pressure, lower reduction temperature.)

The series of IR spectra recorded during stepwise CO adsorption over the annealed 0.5, 2.5 and 10 wt% Pd/γ-Al_2O_3 catalysts at 295 K sample temperature are displayed in panels ***a***, ***b***, and ***c*** of Fig. 2, respectively. Prior to the admission of the first CO aliquot the samples were annealed at 773 K for 2 h in vacuum (P~2×10^{-8} Torr). The CO pressure in the IR cell was increased until an equilibrium pressure of ~0.3 Torr was reached. After the introduction of a very small amount of CO into the IR cell (all the CO was adsorbed) a broad and two sharp IR features appear in the bottom spectrum (black) in panel ***a*** of Fig. 2, representing the C-O stretching vibrations of bridging (1967 cm^{-1}) and linear a-top CO (2116 cm^{-1}) on Pd^+ and a-top CO on Pd^{2+} ions (2130-2160 cm^{-1}), respectively (Table S1 summarizes the IR peak assignments of CO adsorbed on Pd). These assignments were based on prior studies [18-23] on similar systems (tabulated peak assignments can also be found in Refs. 20 and 21). The assignment of the 2130-2160 cm^{-1} band to a-top CO on Pd^{2+} ions is well established in prior literature [18-23]. On the other hand, the assignments of the 1967 cm^{-1} feature to CO adsorbed on bridge sites of Pd^+ and the 2116 cm^{-1} band to linear a-top CO on Pd^+ are not without ambiguity. The spectral region where the 1967 cm^{-1} feature is located at is characteristic, in general, to CO adsorbed in bridge configuration. In most studies this band has been assigned to bridge-bound CO on Pd^0 [20-22,24,25], however, there are some reports that propose the assignment of this feature to CO bridge-bound to Pd^+ species [20], based on organometallic analogues. Similarly, the 2116 cm^{-1} IR feature has also been suggested to represent CO molecules in a-top positions on Pd^0 sites [26]. In a model Pd/Al_2O_3 catalyst system Wolter et al., [26] observed a sharp IR band at 2100-2116 cm^{-1} at 90 K, which they assigned to a-top bound CO on Pd^0. (From our work the definitive assignments of these two features to CO adsorbed either to Pd^0 or Pd^+ cannot be made, however, our data seems to be more consistent with assignment of these bands to CO adsorbed onto charged Pd species. Therefore, throughout the rest of the discussion on CO adsorption at 295 as well as 100 K we will follow these assignments.) The introduction of the second (small) CO aliquot resulted in the intensity gains of all of these features, and no other change in the IR spectrum. After the addition of the third CO aliquot, concomitant to the further intensity gains of these IR features, the appearances of new IR bands were observed in the 1100 – 1850 cm^{-1} region, and also at $\nu>2200\ cm^{-1}$. IR features in the low frequency range resemble those we have reported after CO_2 adsorption on both pure γ-Al_2O_3 and Pd/γ-Al_2O_3, namely carbonates and bicarbonates in the 1100-1850 cm^{-1} spectral range. The high frequency feature centered at around 2240 cm^{-1} represents CO molecules adsorbed on defect sites (Lewis acidic Al^{3+} surface ions) on the partially dehydroxylated alumina support. The intensities of all these IR features increase gradually with increasing amounts of CO in concert with the increasing CO coverage on oxidized Pd, and CO_2 accumulation (formation of carbonates and bicarbonates) on the alumina support. The intensity of the 1967 cm^{-1} IR feature reaches its maximum at an intermediate CO dosage, and then it drops to nearly zero as the amount of CO introduced into the IR cell increased further. This observation is consistent with the well known coverage dependence of adsorbed CO configuration on precious metal surfaces: at low coverages CO binds to two (bridge) or three (free-fold hollow) metal atoms; however, with the increase in CO coverage the surface cannot accommodate these multiple binding configurations, and the CO is forced to occupy an on-top, linear configuration [28,29]. With increasing CO coverage distinct IR features at $\nu>2170\ cm^{-1}$ appear, and can be assigned to CO adsorbed on different defect sites on alumina. It is also clear from these IR data that Pd in the 0.5 wt% Pd/γ-Al_2O_3 catalyst is present exclusively in ionic (in +1 and +2 oxidation states) form following the 773 K annealing (remember that the sample was calcined in O_2 flow *ex situ* prior to mounting it into the IR cell). The most interesting aspect of the spectra of panel ***a*** of Fig. 2 is the development of IR features characteristic of carbonates and bicarbonates on the alumina support. These features are completely absent from the pure alumina when it is exposed to CO only. Therefore, the formation of carbonates and bicarbonates must be related to the presence of Pd on the alumina support. Note, that with increasing CO coverage weak IR bands (shoulders on the low frequency side of the 2116 cm^{-1} feature) of metallic Pd-adsorbed CO develops, suggesting that CO is able to reduce the supported PdO species even at room temperature, as has been suggested by Zorn et al. [25]. We do not believe that a "water gas shift reaction" type of mechanism [14] is in affect here, rather CO is reducing the supported PdO particles to from $Pd^{\delta+}$ and Pd^0. The reduction of oxide supported Pd^{n+} ions by CO at ambient temperatures has been reported by Vijayanand et al. [30] who claimed sequential reduction of Pd^{3+} to Pd^{2+}, Pd^+ and even to Pd^0 over Pd/WO_3-ZrO_2 catalysts. Also note the sharpness of the IR bands of linearly adsorbed CO features in this series of IR spectra indicating the very uniform distribution of carbonyl configurations that arises from the high dispersion of Pd on the alumina support. This is consistent with our TEM observation from this sample that indicated the presence of mostly atomically dispersed Pd species after calcination [9].

The series of IR spectra recorded during CO adsorption on an annealed 2.5 wt% Pd/γ-Al_2O_3 sample at 295 K is displayed in panel ***b*** of Fig. 2. The IR features observed are very similar to those we have just discussed for the 0.5 wt% Pd-containing catalyst, however significant differences need to be pointed out. At low CO coverages (bottom six spectra) the IR features observed on this sample are identical to those we have seen for the 0.5 wt% sample in panel ***a***; bridged and a-top CO on Pd^+ (1966 and 2117 cm^{-1}, respectively), and a-top CO on Pd^{2+} (2130-2160 cm^{-1}). Even in the presence of only very small amount of CO we can clearly observe the formation of carbonates and bicarbonates on the alumina support (IR features in the 1100-1850 cm^{-1} region in the bottom four spectra). With increasing amount of CO introduction into the IR cell the intensities of all of these IR features increase simultaneously (from the 5th spectrum to the 9th), and bands representing CO molecules adsorbed onto the defect sites on the alumina support appear as well (ν>2170 cm^{-1}). Above this CO coverage (last three spectra) the most important change in the IR spectra is the disappearance of the 1966 cm^{-1} band, and the subsequent development of two new features at 1931 and 1981 cm^{-1}. The disappearance of the 1966 cm^{-1} IR feature can be caused either by the change in adsorption configuration as the amount of CO present in the IR cell increases (i.e., conversion of the bridge-bound CO to on-top CO on Pd^+), or the reduction of Pd^+ to Pd^0, and the adsorption of CO on the thus formed metallic Pd, or most probably both. As the surface of the PdO particles becomes reduced (as a result of CO exposure), bridged (1981 $cm^{-1}$and 1931 cm^{-1}) carbonyl species can form on different facets of the Pd crystallites. The ongoing reduction is manifested itself in the large intensity gains of all the carbonate and bicarbonate features. The formation of these metallic species was not evident in the case of the 0.5 wt% Pd/γ-Al_2O_3 sample, suggesting that the reducibility of the very highly dispersed Pd particles on the alumina surface is lower than that of 3D particles. It is also interesting to note when we compare the two sets of IR spectra from the annealed 0.5 and 2.5 wt% Pd/γ-Al_2O_3 samples that IR bands of adsorbed CO are much sharper for the low Pd-loaded sample. This suggests a much more uniform distribution of adsorption sites at low Pd loading, and conversely, the much more heterogeneous site distribution on the higher loaded sample where the presence of 3D clusters provide a wealth of adsorption sites on terraces, edges, kinks, etc.

The series of IR spectra obtained from the annealed 10 wt% Pd/γ-Al_2O_3 catalyst at 295 K is very different from those recorded from the two low Pd-loaded samples under identical conditions (panel ***c*** of Fig. 2). The most striking feature of this spectral series is the presence of intense absorption features at 1932-1951 and 1974-1989 cm^{-1}, characteristic of bridge-bound CO on metallic Pd surfaces [19-22, 28]. The IR feature at around 1935 cm^{-1} may have contribution from bridged CO on $(Pd^+)_n$ ions as it was suggested by Xu and co-workers [31]). This is supported by the fact that at the lowest CO exposures (spectra a-c) this is the dominant feature in the 1900-2000 cm^{-1} spectral region. It is also evident, just as we have seen for the 2.5 wt% Pd-loaded sample, that CO_2 forms even at very low CO levels, resulting in the appearances of IR features characteristic of carbonate and bicarbonate species bound to the alumina support. With increasing amount of CO introduced, the intensity of the IR band at 1974-1989 cm^{-1} increases much faster than that of the band at around 1935 cm^{-1}, due, most probably, to the formation of reduced Pd surface sites. The relative intensities of the linearly bound CO onto Pd^+ (2117-2110 cm^{-1}) and Pd^{2+} (2130-2155 cm^{-1}) ions are much lower than in the case of the low Pd-loaded samples in panels **a** and **b**. The facile reduction of the PdO particles by CO at 295 K is manifested not only in the formation of intense carbonate and bicarbonate features, but also by the appearance of a new IR feature centered at 2367 cm^{-1}, representing CO_2 adsorbed on defect sites of the alumina support.

Next we investigated the adsorption of CO on the three oxidized Pd/γ-Al_2O_3 catalysts at 295 K. The oxidation was carried out in two steps: first the sample was kept at 573 K in ~0.4 Torr of O_2 for 10 min, and then the cell was evacuated while the sample temperature was constant at 573 K.

Following the second oxidation step (under identical conditions to the first one) the sample was cooled to below 300 K before the cell was evacuated in order to minimize the possibility of autoreduction of PdO in high vacuum at elevated temperatures. After the pressure in the IR cell dropped below ~2×10^{-8} Torr, CO adsorption was conducted in the same way as we have discussed it above for the annealed samples. Since the main characteristics of the IR spectra for these three oxidized samples were similar to those we discussed above for the annealed ones the results obtained from these systems are shown in the Supplementary Information. The three series of IR spectra collected during stepwise CO adsorption from the oxidized 0.5, 2.5 and 10 wt% Pd/γ-Al_2O_3 samples at 295 K are displayed in panels ***a***, ***b***, and ***c*** of Fig. S1, respectively. The C-O stretching vibrational region of the IR spectra obtained from the oxidized 0.5 wt% Pd/γ-Al_2O_3 sample dominated by a sharp feature centered at around 2140 cm^{-1}, with a shoulder developing at higher CO exposure at ~2085 cm^{-1}. This intense band is assigned to CO adsorbed onto Pd^{2+} surface sites, indicating that under the oxidation conditions applied all the Pd have been converted to Pd^{2+} ions. At higher CO exposures the development of the ~2085 cm^{-1} shoulder, as well as the appearance of a broad, low intensity feature between 1900 and 1970 cm^{-1} indicates the formation of both Pd^{+} and Pd^{0} centers as CO reduces some of the Pd^{2+} sites. Concomitant to the appearance of Pd^{+}-and Pd^{0}-adsorbed CO bands is the development of IR bands characteristic of alumina-bound carbonate and bicarbonate species in the 1100 – 1850 cm^{-1} spectral range. The intensities of these carbonate and bicarbonate species relative to the Pd^{n+}-bound CO peak are much higher on the oxidized sample than on the annealed one (Fig. 2***a***), consistent with the presence of a larger oxygen “pool” on the oxidized sample. The main features of the IR spectra of oxidized 2.5 wt% Pd/γ-Al_2O_3 are very similar to that we have discussed for the corresponding annealed sample. In contrast to the 0.5 wt% sample a large fraction of the Pd ions is present in 1+ instead of 2+ oxidation state, and as the CO exposure is increased the formation of metallic Pd is seen as well (note the at low CO exposure the broad IR feature has a maximum intensity at 2114 cm^{-1}, representing CO molecules adsorbed onto Pd^{+} ions, while at high CO exposure this features becomes much broader and contain contributions from CO adsorbed on both Pd^{+} and Pd^{0}). The extent of PdO reduction in the presence of CO is evidenced by the development of intense carbonate and bicarbonate features in the 1100 – 1850 cm^{-1} spectral range. Note also the development of an IR band at 2367 cm^{-1} of adsorbed CO_2

bound to defect sites on the alumina support. As the defect sites are occupied primarily by CO_2, the intensity of defect site-bound CO features (2240 and 2218 cm^{-1}) strongly decrease (in comparison to the annealed sample). The intensity ratios of the CO features bound to Pd in different oxidation states (0, 1+ and 2+) on the oxidized 10 wt% Pd/γ-Al_2O_3 sample change significantly in comparison the those on the annealed sample. The most important difference between the two sets of IR spectra (Fig. S2c and Fig. 2c) is the much higher intensities of the Pd^+ and Pd^{2+}-bound CO species on the oxidized sample. Similarly to the annealed sample the Pd^0-bound CO features (1984-1994 and ~1950 cm^{-1}) have high intensities even from the onset of CO exposure. These results suggest that either the oxidation conditions applied here were not sufficient to oxidize all the Pd species into Pd^{2+}, or the PdO particles formed in the oxidation were partially reduced by reducing environment of the high vacuum following the oxidation step. The oxide species formed at low Pd loadings (0.5 and 2.5 wt%) seem to be much less susceptible to reduction either by high vacuum or by CO than the 10 wt% Pd-loaded sample. The large amount of CO_2 formed upon the interaction of CO with the oxidized 10 wt% Pd/γ-Al_2O_3 sample is also evidenced by the development of the 2365 cm^{-1} feature of defect site-adsorbed CO_2. (In fact the amount of CO_2 formed over this sample is large enough to completely suppress the adsorption of CO on these defect sites; i.e., no IR features are observed at 2240 and 2220 cm^{-1}.

The adsorption of CO was also investigated on the H_2 reduced samples at 295 K. After completion of the CO adsorption experiments the oxidized sample was annealed at 773 K for 2 h, and then reduced with H_2 (0.4 Torr) at 573 K for 10 min two times. After the second reduction step the IR cell was evacuated and the sample was annealed again at 773 K for 30 min, then cooled down to 295 K for the adsorption experiment. The three sets of IR data obtained after the room temperature CO adsorption on the reduced 0.5, 2.5 and 10 wt% Pd/γ-Al_2O_3 samples are shown in panels ***a***, ***b*** and ***c*** of Fig. 3., respectively. Somewhat surprisingly, the most intense IR features observed in the IR spectra of the reduced, 0.5 wt% Pd/γ-Al_2O_3 sample up to moderate CO exposures are the ones representing CO molecules adsorbed onto Pd^+ centers (peaks at 2116-2114 and 1966 cm^{-1}). The other features in the CO vibrational region originate from CO adsorbed onto metallic Pd (bands at 2098, 2072 cm^{-1} (linear a-top CO) and the broad band centered around 1920 cm^{-1} (bridge bound CO)). With increasing CO exposure the intensities of all IR features increase, although with not the same rate. In particular, the intensity of the band at 1966 cm^{-1} increases up to an intermediate CO exposure, and then it decreases. This observation can be explained by the changing adsorption geometry as the CO coverage increases and/or by the reduction of the Pd^+ adsorption centers by CO at elevated pressures. We believe that both of these processes contribute to the observed variation in the intensity of the 1966 cm^{-1} IR feature. The reduction of the oxidized Pd adsorption centers is evidenced by the appearance and subsequent development of IR bands of carbonate/bi-carbonate species on the alumina support (peaks in the 1100-1800 cm^{-1} range). The IR spectra also reveal that a small number of Pd^{2+} adsorption sites are present in this sample (IR band at 2155 cm^{-1}) even after the reduction treatment applied. The series of IR spectra (panel ***b*** of Fig. 3) obtained from the reduced 2.5 wt% Pd/γ-Al_2O_3 sample indicate that most of the Pd adsorption sites are present in metallic state, and only very small amount of Pd^+ sites exists. The most intense feature is centered at 2093-2098 cm^{-1} and represents a-top-bound CO molecules on Pd^0 adsorption centers. The weak shoulder (at 2113 cm^{-1}) on the high frequency side of this band at low CO exposures substantiates that not all the surface Pd sites were reduced by the relatively mild reduction process applied. The presence of a small number of Pd^+ centers is also suggested by the development of a weak IR band at 1966 cm^{-1}, especially at low CO exposures. The intensity of this feature seems to decrease as the amount of CO introduced into the IR cell increases. This is due, most probably, by the reduction of the Pd^+ sites at higher CO partial pressures evidenced by the appearance of weak bands of carbonates and bicarbonates bound to the alumina support. The IR spectra collected from the CO-exposed reduced 10 wt% Pd/γ-Al_2O_3 sample (panel ***c*** of Fig. 3) shows the presence of metallic Pd only in this sample. All the IR features observed represent Pd^0-bound CO species in different adsorption geometries: a-top (2082, 2095-2099 cm^{-1}) and bridged (1940-1990 cm^{-1}). The very sharp features observed on this sample can be attributed to the formation of large crystalline Pd particles exhibiting well defined crystal facets. The IR bands of adsorbed CO on this sample can be assigned to specific crystal faces: linear CO on Pd(111) (2095-2099 cm^{-1}) and Pd(100) (2082 cm^{-1}), bridge-bound CO on Pd(111) 1939-1948 cm^{-1}) and Pd(100) (1970-1990 cm^{-1}) [28]. The almost complete absence of alumina-bound carbonate and bi-carbonate features further substantiates the high level of reduction of this sample.

Comparing the results obtained from the reduced Pd/γ-Al_2O_3 samples (reduction was carried out under the same experimental conditions on all three samples) at different Pd loadings clearly indicate that reduction efficiency increases with increasing Pd loading. We attribute this observation to the strength of metal – support interaction at different Pd loadings. In the low Pd-loaded sample (0.5 wt%) most of the metal is present in very high dispersion, and the interaction of the small metal particles and atoms with the alumina support is strong. As we have discussed it previously, the Pd atoms (ions) are connected to the alumina support through an oxygen bridge, and the reduction of the thus bound Pd ions is difficult, therefore, a significant fraction of Pd remains in the oxidized state even after reduction. In contrast, Pd is mainly present as part of large particles (several nm), and most of the surface Pd atoms are not bound to the alumina surface, and, consequently, can readily be reduced to metallic state with H_2. Another interesting observation from data presented in Fig. 2 is the ability of CO to reduce some of the Pd ions at room temperature, thus produce CO_2 that, in turn, can form carbonates and bi-carbonates on the alumina support. In agreement with the discussion above about the dependence of reducibility on Pd dispersion, the clearest evidence for carbonate/bi-carbonate formation is seen on the sample with the lowest metal loading (0.5 wt%), while practically no CO_2 formation can be deduced from the IR data presented for the 10 wt% Pd/γ-Al_2O_3 sample. The IR data collected from these reduced samples also provide clear evidence for the decreasing metal dispersion with increasing Pd loading. While the IR feature of a-top-bound CO (2000-2150 cm^{-1}) is the most intense on the 0.5 wt% Pd/γ-Al_2O_3 sample, as the Pd loading increases the intensity ratio of the bridge/a-top-bound CO features increases dramatically. In the IR spectra of adsorbed CO on the 10 wt% Pd/γ-Al_2O_3 sample most of the CO are present in bridged configurations on well defined crystal facets.

The last point we need to discuss here is the formation of carbonates/bicarbonates on these Pd/γ-Al_2O_3 samples following different pre-treatments (annealing, oxidation, reduction). In all three annealed and oxidized samples (0.5, 2.5 and 10 wt% Pd) we observed the development of very intense IR features of bicarbonates after CO exposure. We attributed (see discussion above) the formation of these surface species to the production of CO_2 by the reduction of surface PdO_x with CO, and its subsequent reaction with the alumina support. The intensities of the IR bands representing these bicarbonate species were always higher on the oxidized samples than on the annealed ones. This observation is in concert with the extent of oxidation of the Pd particles following the two different pretreatments; i.e., a larger fraction of the Pd phase is present as an oxide in the oxidized sample than in the annealed one (as evidenced by the higher intensity of the IR features of adsorbed CO on Pd^{2+} after oxidation). The almost complete absence of bicarbonates on all three reduced samples supports our hypothesis that the formation of bicarbonates requires the presence of CO_2. This conclusion is in contrast to that of Föttinger et al. [14], who have reported the formation of these bicarbonates on both γ-Al_2O_3 and Pd/γ-Al_2O_3 samples in the presence of CO only. As we have discussed in our prior work on the interaction of CO and CO_2 with a γ-Al_2O_3 support, we observed the formation of bicarbonates only when CO_2 was introduced onto the sample, but never with CO alone, regardless of sample pretreatment (annealing, oxidation, reduction). These observations are even more intriguing in light that the γ-Al_2O_3 support studied by Föttinger et al. [14], and by us were from the same source (Puralox SBA 200). In the complete absence of either CO_2 (in the case of the alumina support) or surface oxygen on the Pd phase (in case of the Pd/γ-Al_2O_3 samples) no evidence for carbonate/bicarbonate formation was observed on our samples. In the report by Föttinger et al. [14] no data in the vibrational region where Pd- and PdO_x-adsorbed CO could be seen was shown, and therefore we can not speculate on the presence or absence of any Pd-oxide that could be responsible for the formation of CO_2 upon CO exposure. (Although in their follow-up study [27] the IR spectrum they obtained from CO exposed Pd/Al_2O_3 seems to show no evidence for CO adsorbed on ionic Pd sites.) On the other hand, even if some Pd-oxide is present on their sample we could still not explain their observation of bicarbonate formation from CO on the alumina support alone. At this point we have no explanation for these contradicting observations, only the fact that we could only observe the formation of bicarbonates when CO_2 was present (even if in trace amounts). On the other hand, our conclusion is in full agreement with that of Morterra et al., who reported the complete lack of carbonate/bicarbonate formation on a series of pure transition aluminas in the presence of CO alone [12].

3. CO adsorption at 100 K: In order to minimize reaction between CO and the Pd/PdO_x particles, we have also conducted CO adsorption experiments on these three (0.5, 2.5 and 10 wt%) Pd/γ-Al_2O_3 samples at 100 K. Here we report the results obtained from the oxidized and reduced samples, since the IR spectra obtained from the annealed samples showed very similar characteristics to those recorded from the oxidized ones (just as we have discussed above for the 295 K adsorption). Prior to CO exposure the samples were heated in O_2 at 573 K for 10 min two times. After the first oxidation the IR cell was evacuated while the sample was kept at 573 K. However, after the second oxidation step (under the same conditions as the first one) the sample was cooled to 300 K and evacuated until the pressure in the IR cell dropped below $5x10^{-8}$ Torr. Then the sample was cooled to and kept at 100 K and stepwise CO adsorption experiments were carried out. The reduced samples were prepared by reduction in H_2 at 573 K two times. After the first reduction step the sample was kept at the reduction temperature during evacuation, while following the second reduction the sample was heated to 773 K during evacuation, and kept at that temperature for 30 min. Then the sample was cooled to 100 K for CO adsorption. After the completion of CO adsorption on both the oxidized and reduced samples stepwise annealing was carried out, and after each annealing step the sample was cooled back to 100 K and an IR spectrum was acquired. (Since absorption features of the weakly held, alumina support-bound CO dominated the IR spectra collected during CO adsorption at 100 K, discussion on the series of IR spectra collected from these samples are presented in the Supplementary Information (Figures S3-S8). Here we discuss in details the results of the step-wise annealing experiments.)

The series of IR spectra collected during the stepwise annealing (from 100 to 300 K) of the CO-saturated, oxidized 0.5 wt% Pd/γ-Al_2O_3 sample is shown in panel **a** of Fig. 4. The intense IR features of the support bound, weakly held CO are not shown in order to make it easier to observe the variation in the IR features representing Pd-related adsorbed CO. In the top spectrum of this (CO adsorption at 100 K) we can clearly see the presence of weak, broad bands representing weakly held carbonates (1850-1750 cm^{-1}), and even perhaps some adsorbed CO on $Pd^{\delta+}$ (1850-1950 cm^{-1}). Heating the CO–saturated sample to 160 K (fourth spectrum from the top) results primarily in desorption of hydrogen-bonded CO (the broad feature in the 3400-3650 cm^{-1} region completely disappears), and the development of IR features of surface carbonates (1750-1875 cm^{-1}) on alumina. In this spectrum the broad band centered at ~2140 cm^{-1} (and was present only as a shoulder at saturation CO exposure) is present with high intensity, and represent CO adsorbed mainly onto Pd^{2+} (higher frequency part of the feature) and, in a lesser extent, to Pd^{+} (lower frequency range of this feature) sites [21]. No evidence for other Pd-related CO features can be seen. These observations indicate that the 0.5 wt% Pd/γ-Al_2O_3 sample contain only ionic Pd species after oxidation, and during CO adsorption at 100 K. (The broadness of the feature at 2140 cm^{-1} already suggests the onset of reduction of Pd^{2+} to Pd^{+} ions, which is also substantiated by the intensity gain of the surface carbonate features at 1850-1750 cm^{-1}.) Further heating the sample to 180, then 200 K clearly shows the reduction of the Pd^{2+} ions by CO, evidenced by the appearance and intensity gain of the IR feature at 2108 cm^{-1}, and the further intensification of the carbonate features. After annealing the sample to 225 K (fourth spectrum from the bottom) the most intense CO band (2108 cm^{-1}) is the one representing CO linearly bonded to Pd^{+}. There is also a definite intensity gain at around 1995 cm^{-1} which also indicates the formation of metallic Pd as a result of reduction of PdO_x. At this temperature the appearance of IR features of bicarbonates (1236, 1494. 1648 cm^{-1}) bound to the alumina support is also apparent. Increasing the annealing temperature to 250, 275 and finally 300 K results in further intensity drop of the ~2140 cm^{-1} band, and the marked increase in the intensity of the IR features at 1942 and ~1995 cm^{-1}. These observations are consistent with the reduction of surface oxides by CO, and the subsequent adsorption of CO on the thus formed metallic and $Pd^{\delta+}$ sites. As the reduction of PdO_x proceeds, i.e., CO_2 forms, the alumina-bound bicarbonates gain further intensity. (Since these experiments are carried out under dynamic vacuum the amount of CO present in the system during the stepwise temperature ramp is not constant. The two key processes taking place are desorption of weakly held CO and reaction of CO with PdO_x to from CO_2. The thus formed CO_2 either desorbs or interacts with the alumina support to form carbonates/bicarbonates.) The fact that after the final annealing step to 300 K the most intense features are the ones that represent CO linearly and bridge-bound to metallic Pd indicate the very high dispersion of PdO_x species after the oxidation step. This observation is consistent with the recent findings of Gaudet et. al., who observed (by TEM) the formation of highly dispersed PdO_x species upon the oxidation of Pd/γ-Al_2O_3 catalysts [32].

The IR spectra collected during the stepwise (each step is 25 K) annealing of the CO-saturated, reduced 0.5 wt% Pd/Al_2O_3 sample from 125 to 300 K are shown in panel ***b*** of Fig. 4 (again we do not show the entire absorbance scale in order to focus on the variation of the intensities of CO adsorbed on Pd). In the spectrum collected after annealing the sample to 150 K we can clearly see the presence of Pd^{2+} ion-bound CO (2145 cm^{-1}), although most of the CO is adsorbed onto metallic Pd in linear (2107-2100 cm^{-1}) and bridge-bound (2000-1850 cm^{-1}) configurations. In the temperature range of 150-225 K the small amount of Pd^{2+}-bound CO completely disappears, and concomitantly a new feature develops at 2120 cm^{-1} representing CO linearly adsorbed to Pd^{+} sites. Interestingly, no IR features of alumina-bound carbonates/bicarbonates can be observed during this reduction, most probably due to the removal of the small amount of CO_2, formed during the reduction, by the dynamic evacuation. Heating the sample from 225 to 300 K results, mostly, in the intensity variation of the metallic Pd-bound linear and bridged CO features, and in some intensity loss of the Pd^{+} bound linear CO feature. As more Pd^{0} sites form (due to reduction with CO) increasing fraction of the adsorbed CO can be accommodated in bridge-bound configuration, instead of the linear one. Note that in the entire annealing process up to 300 K no carbonate/bicarbonate formation was observed at all, in stark contrast to that observed for the oxidized 0.5 wt% Pd/γ-Al_2O_3 sample.

The changes in the IR spectra collected during stepwise annealing (25 K/step) of the CO-saturated, oxidized 2.5 wt% γ-Pd/Al_2O_3 sample are very similar to those we have shown in the previous paragraph for the 0.5 wt% Pd/γ-Al_2O_3 sample (panel ***a*** of Fig. 5). Specifically, upto 175 K there is only a very limited extent of PdO reduction, and consequently the formation of bridging carbonates on the alumina support solely. In the spectrum obtained after annealing the sample to 175 K we can see the appearance of a shoulder around 2105 cm^{-1}, indicating the presence of Pd^{0} species. The spectrum recorded after the 200 K annealing step clearly shows the new IR feature at ~2105 cm^{-1}, and also the appearances of IR bands of bicarbonate species (1645, 1490 and 1238 cm^{-1}). The IR feature at 2140 cm^{-1} is rather broad, due, possibly to the overlap of vibrational features arises from CO adsorbed on both Pd^{2+} and Pd^{+} ions. In the 200 to 300 K annealing temperature range the 2140 cm^{-1} feature loses most of its intensity, and CO is adsorbed primarily to Pd^{0} sites in linear configuration (2105-2096 cm^{-1}). Some CO is also occupying bridge bound configurations, as the intensity increase of the IR feature at 1982 cm^{-1} indicates. Due to the presence of more Pd in this sample in comparison to the 0.5 wt% one, the amount of CO_2 formed is much higher here. This is the reason for the formation of not only the high intensity bicarbonate features, but the sharp band at 2366 cm^{-1} of CO_2 linearly adsorbed onto the alumina support.

The series of IR spectra collected during the stepwise annealing of the CO-saturated (at 100 K), reduced 2.5 wt% Pd/γ-Al_2O_3 sample is shown in panel **b** of Fig. 5. Beside the bands of the alumina-related adsorbed CO (2197-2188 and 2166-2163 cm^{-1}) all the other IR features observed during CO adsorption are the ones that represent CO molecules on metallic Pd in linear (2107 cm^{-1}) and bridge (1991, 1958 and 1890 cm^{-1}) configurations. Interestingly, in the IR spectra collected during the annealing process we do not observe any evidence for the presence of Pd^{2+} adsorption centers, and only a very weak shoulder at 2120 cm^{-1} indicating the existence of some Pd^{+} centers. However, it is clear from the data presented here that reduction of the 2.5 wt% Pd/γ-Al_2O_3 sample is much more complete that that of the 0.5 wt% one. Similarly to the reduced 0.5 wt% sample the formation of neither carbonates nor bicarbonates was observed on the reduced 2.5 wt% sample.

The IR spectra (panel **a** of Fig. 6) collected during stepwise annealing following low temperature CO adsorption on the oxidized 10 wt% γ-Pd/Al_2O_3 sample show similar trends to the other, lower Pd-loaded oxidized samples up to 175 K. In the 100-175 K temperature region alumina-bound, weakly held CO is removed primarily, and also the intensities of bridging carbonates increase as some of the Pd^{2+} is reduced to Pd^{+}, and perhaps even to Pd^{0}. After annealing to 200 K (fifth spectrum from the top) the distinct IR band of linear CO on Pd^{0} appears (2107 cm^{-1}) and also the IR signatures of alumina-bound bicarbonates become visible. The broad IR feature between 2000 and 2180 cm^{-1} at this temperature represents linearly adsorbed CO molecules on Pd species in all three (0, +1, and +2) oxidation states. Most of the Pd CO bound to is still in the oxidized state, mainly in the form of Pd^{2+}. The broad band centered around 1970 cm^{-1} belongs to bridged CO molecules on Pd^{2+} ions. As the annealing temperature gradually increased in 25 K increments to 300 K the IR feature of Pd^{2+}-bound CO decrease, but even after 300 K annealing there is a significant intensity of the band at ~2150 cm^{-1} (still a lot of ionic Pd is present on the surface). The intensity of the IR feature of linearly bonded CO on Pd^{0} increases initially, but above 250 K annealing temperature it loses significant portion of its intensity, and the Pd^{0}-bound CO is mostly present in bridged configuration. The amount of CO_2 produced during the annealing process (as a result of PdO_x reduction) is large enough not only to produce carbonate and bicarbonate species, but also to allow some of the CO_2 to adsorb onto the alumina support (2366 cm^{-1} IR feature).

The series of IR spectra obtained from the reduced 10 wt% Pd/γ-Al_2O_3 sample at 100 K (Fig. S7) during step-wise CO adsorption suggests that Pd is only present in metallic state. The high intensity, sharp IR features of linearly (2106 cm^{-1}) and bridge (1890, 1958, 1997 cm^{-1}) bonded adsorbed CO indicate the formation of rather large metal particles with well ordered crystal facets during reduction in H_2 at 573 K, and subsequent annealing at 773 K. The series of IR spectra collected during annealing from 100 to 300 K reveals the complete absence of any ionic Pd adsorption centers (panel **b** of Fig. 6). As a result of this annealing process the only change taking place in this sample is the variation of the ratio of a-top- to-bridge-bound CO. After annealing this reduced sample to 300 K CO is mostly present in bridge-bonded configuration on low index, (111) and (100), Pd crystallite facets. Since no oxidation reaction took place during annealing, i.e., no CO_2 was produced, neither the IR features of carbonates/bicarbonates nor that of adsorbed CO_2 is observed. These observations are in agreement with our earlier conclusion: larger oxidized metal particles (present in 10 wt% Pd/γ-Al_2O_3) are easier to fully reduce than highly dispersed ones (in 0.5 wt% Pd/γ-Al_2O_3). This is most probably due to the strong influence of the alumina support on the metal particles at very high dispersions.

The results of these low temperature CO adsorption studies clearly show that regardless of Pd loading (in the 0.5 to 10 wt% range) oxidation at 573 K can convert all the metal into PdO. (In light of a recent study by Zorn at al., [25] we cannot exclude the possibility that Pd particles after the relatively mild oxidation step applied in this work are only partially oxidized, i.e., PdO^x shell surrounding the metallic Pd core. Most of the results presented here are consistent with those reported by Zorn et al., except the assignment of the 2145 cm^{-1} band in the IR spectrum. In Ref. 25 this feature was assigned to CO linearly adsorbed onto $Pd^{\delta+}$, while our results are more consistent with the assignment of this feature to CO linearly bound to Pd^{2+} ions. This assignment is also consistent with those of Martin at al., [22], Tessier et al., [20] and Tiznado et al., [21].) On the other hand, treatment in H_2 at 573 K is not sufficient to reduce all the Pd ions at high Pd dispersions. However, when Pd is present in large particles (like in the 10 wt% Pd/γ-Al_2O_3 sample) all the Pd ions are reduced to Pd^0. These results also suggest that using CO adsorption to determine the number of surface Pd sites (Pd dispersion) is not suitable when the sample is not fully oxidized. In (partially) oxidized sample some of the CO introduced to probe Pd sites is consumed in the reduction process, and the thus formed CO_2 may bind to the alumina support either as carbonate/bicarbonate or adsorbed CO_2. This reaction results in the over-estimation of the actual metal dispersion, a conclusion that was advocated by Föttinger et al. [14]. In the case of fully reduced samples, however, this is not a concern, and CO adsorption can be used to accurately probe the number of metallic surface sites.

Conclusions: The adsorption of CO_2 and CO was investigated on three Pd-loaded alumina samples (0.5, 2.5 and 10 wt% Pd loadings) by *in situ* transmission FTIR spectroscopy at 300 and 100 K. The aim of this work was to identify the nature of adsorbed species formed in the adsorption processes over these materials that will aim our ongoing research to understand the reaction mechanism of CO_2 reduction. We were also interested in following the oxidation state variation of the active metal (Pd) as a function of sample treatment conditions (annealing, reduction and oxidation) utilizing the sensitivity of the C-O stretching vibrational frequency to both the electronic state and coordination environment of the adsorption sites. Exposing the annealed Pd/Al_2O_3 samples to CO_2 at 295 K produced only the same surface species we have observed upon CO_2 exposure of the metal-free alumina support: weakly held, adsorbed CO_2, bidentate carbonates and bicarbonates. The IR spectra recorded after CO exposure of the oxidized, annealed and reduced samples displayed characteristic features of both metallic and ionic Pd-bound CO, as well as bands that were seen after CO_2 adsorption, i.e., adsorbed CO_2, carbonates/bicarbonates. The intensities of all these bands were dependent upon both the Pd loading, and the pretreatment of the catalyst (oxidation, annealing, reduction). The appearance of IR features associated with CO_2 exposure evidences the reduction of PdO_x species by CO even at 295 K. Adsorption of CO at 100 K provided more accurate information about the state of Pd after oxidation and reduction: exclusively oxidized Pd after oxidation, and mostly reduced Pd after reduction. Annealing the samples after low temperature CO exposure clearly showed the progression of reduction of the PdO_x species. This process was initiated at much lower temperature than 300 K, and the reduction efficiency was dependent on the Pd loading. Due to the strong interaction between the metal and the support at high metal dispersions, the 0.5 wt% Pd/Al_2O_3 sample was the most difficult to reduce.

Acknowledgements: The catalyst preparation was supported by a Laboratory Directed Research and Development (LDRD) project. This work was supported by the US Department of Energy Basic Energy Sciences, Division of Chemical Sciences, Geosciences & Biosciences.

Pacific Northwest National Laboratory is operated by Battelle for the US Department of Energy. JHK also acknowledges the support of this work by the 2013 Research Fund of UNIST (Ulsan National Institute of Science and Technology, Ulsan, Korea). The authors also thank Mark Engelhard for conducting the XPS experiments on the Pd-loaded samples.

References:

1. Wang, W., Wang, S., Ma, X., Gong, J., Recent Advances in Catalytic Hydrogenation of Carbon Dioxide**.** *Chem. Soc. Rev.,* **2011**, *40*, 3703–3727.

2. Berkó, A., Solymosi, F., Effects of potassium on the chemisorption of CO_2 and CO on the Pd(100) surface. *Surf. Sci.* **1986**, *171*, L498-502.

3. Solymosi, F., Berkó, A., Adsorption of CO_2 on Clean and Potassium-covered Pd(100) surfaces. *J. Catal.* **1986**, *101,* 458-472.

4. Solymosi, F., Bugyi, L., Adsorption and Dossociation of CO_2 on a Potassium-Promoted Rh(111) Surface. *J. Chem. Soc., Faraday Trans. 1* **1987,** *83,* 2015-2033.

5. Kiss, J., Révész, K., Solymosi, F., Photoelectron spectroscop1c studies of the adsorption of CO_2 on potassium-promoted Rh(111) surface. *Surf. Sci.* **1988**, *207,* 36-54.

6. Liu, Z.M., Zhou, Y., Solymosi, F., White, J.M., Vibrational study of carbon dioxide(1-) on potassium-promoted platinum (111). *J.Phys.Chem.* **1989**, *93,* 4383-4385.

7. Solymosi, F., The bonding, structure and reactions of CO_2 adsorbed on clean and promoted metal surfaces. *J.Mol.Catal.,* **1991**, *65,* 337-358.

8. Freund, H.-J., Roberts, M.W., Surface chemistry of carbon dioxide. *Surf.Sci.Reports*, **1996**, *25,* 225-273.

9. Kwak, J.H., Kovarik, L., Szanyi, J., Heterogeneous catalysis on atomically dispersed supported metals: CO_2 reduction on multifunctional Pd catalysts. *ACS Catal.* **2013,** *3,* 2094-2100.

10. Schalow, T., Brandt, B., Starr, D. E., Laurin, M., Shaikhutdinov, S. K., Schauermann, S., Libuda, J., Freund, H.-J., On the nature of Pd^{n+} surface carbonyl and nitrosyl complexes formed on Pd-promoted tungstated zirconia catalysts. *Phys. Chem. Chem. Phys*. **2007**, *9*, 1347–1361.

11. Park, J.N., McFarland E., A highly dispersed Pd–Mg/SiO_2 catalyst active for methanation of CO_2. *J.Catal.* **2009,** *266,* 92-97.

12. . Morterra, C., Magnacca, G., A case study: surface chemistry and surface structure of catalytic aluminas, as studied by vibrational spectroscopy of adsorbed species. *Catal.Today* **1996,** *27,* 497-532.

13. Padley, M.B., Rochester, C.H., Hutchings, G.J., King F., FTIR Spectrocopic Study of Thiophene, SO_2, and CO Adsorption on Cu/Al_2O_3 Catalysts. *J.Catal.* **1994,** *148,* 438.

14. Föttinger, K., Schlögl, R., Rupprechter, G., The mechanism of carbonate formation on Pd-Al_2O_3 catalysts. *Chem.Comm.* **2008,** 320-322.

15. Kwak, J. H., Hu, J. Z., Mei, D., Yi, C. W., Kim, D. H., Peden, C. H. F., Allard, L. F., Szanyi, J., Coordinatively Unsaturated Al^{3+} Centers as Binding Sites for Active Catalyst Phases of Platinum on γ–Al_2O_3. *Science*, **2009**,*325,* 1670–1673.

16. Mei, D., Kwak, J.H., Hu, J., Cho, S.J., Szanyi, J., Allard, L.F., Peden, C H. F., Unique Role of Anchoring Penta-Coordinated Al^{3+} Sites in the Sintering of γ-Al_2O_3-Supported Pt Catalysts. *J. Phys. Chem. Lett.,* **2010,** *1,* 2688–2691.

17. Kwak, J. H., Mei, D. H., Yi, C. W., Kim, D. H., Peden, C. H. F., Allard, L. F., Szanyi, J., Understanding the nature of surface nitrates in BaO/γ -Al_2O_3 NO_x storage materials: A combined experimental and theoretical study. *J. Catal.* **2009**, *261*, 17–22.

18. Palazov A., Kadinov G., Bonev Ch., Shopov D., Infrared spectroscopic study of the interaction between carbon monoxide and hydrogen on supported palladium, *J.Catal.,* **1982***, 74,* 44-54.

19. Juszczyk W., Karpiski Z., Stanasiuk Z., Zielinski J., Sheu L.-L., Sachtler W.M.H., Characterization of supported palladium catalysts: III. Pd/Al_2O_3; *J.Catal*. **1989,** *120*, 68-77.

20. Tessier D., Rakai A., Bozon-Verduraz F., Spectroscopic study of the interaction of carbon monoxide with cationic and metallic palladium in palladium-alumina catalysts, *J.Chem.Soc. Faraday Trans*., **1992**, *88*, 741-749.

21. Tiznado H, Fuentes S., Zaera F., Infrared study of CO adsorbed on Pd/Al2O3-ZrO2. Effect of zirconia added by impregnation, *Langmuir,* **2004**,*20,* 10490-10497.

22. Martin N.M., Van den Bossche M., Gronbeck H., Hakanoglu C., Zhang F., Li T., Gustafson J., Weaver J.F., Lundgren E., CO adsorption on clean and oxidized Pd(111), *J.Phys.Chem. C,* **2014,** *118*, 1118-1128.

23**.** Hadjiivaniv K.I., Vayssilov G.N., Characterization of oxide surfaces and zeolites by carbon monoxide as an IR probe molecule, *Adv.Catal.,* **2002**, *47*, 307-511.

24. Di Gregorio, Bisson, L., Armaroli, T., Verson, C., Lemaitre, L., Thomazeau, C, Characterization of well faceted palladium nanoparticles supported on alumina by transmission electron microscopy and FT-IR spectroscopy of CO adsorption, *ApplCat. A: General*, **2009,** *352*, 50-60.

25. Zorn K., Giorgio S., Halwax E., Henry C.R., Grönbeck H., Rupprechter, CO oxidation on technological Pd-Al_2O_3 catalysts: oxidation state and activity, *J.Phys.Chem. C*, **2011,** *115*, 1103-1111.

26. Wolter K., Seiferth O., Libuda J., Kuhlenbeck H., Baumer M., Freund H.-J., Infrared study of CO adsorption on supported palladium particles, *Surf.Sci.,* **1998**, *402-404,* 428-432.

27**.** Weilach, Ch., Spiel, Ch., Föttinger, K., Rupprechter, G., Carbonate formation on Al_2O_3 thin film model catalyst supports. *Surf.Sci*. **2011,** 605, 1503-1509.

28. Szanyi, J., Kuhn, W.K., Goodman, D.W., CO adsorption on Pd(111) and Pd(100): Low and high pressure correlations. *J.Vac.Sci.Technol. A* **1993***, 11,* 1969-1974**.**

29. Loffreda, D., Simon, D., Sautet, P., Dependence of stretching frequency on surface coverage and adsorbate–adsorbate interactions: a density-functional theory approach of CO on Pd (111). *Surf.Sci.* **1999***, 425,* 68-80.

30. Vijayanand, P., Chakarova, K., Hadjiivanov, K., Lukinskas, P., Knözinger, H., On the nature of Pd^{n+} surface carbonyl and nitrosyl complexes formed on Pd-promoted tungstated zirconia catalyst. *Phys.Chem.Chem.Phys*. **2003**, *5*, 4040-4044.

31. Xu, J., Ouyang, L., Mao, W., Yang, X.-J., Xu, X.-C., Su, J.-J., Zhuang, T.-Z., Li, H., Han, Y.-F., Operando and Kinetic Study of Low-Temperature, Lean-Burn Methane Combustion over a Pd/γ-Al_2O_3 Catalyst. *ACS Catal*., **2012,** *2*, 261–269.

32. Gaudet, J.R., de la Riva, A., Peterson, E.J., Bolin, T., Datye, A.K., Improved Low-Temperature CO Oxidation Performance of Pd Supported on La-Stabilized Alumina. *ACS.Catal.* **2013,** *3*, 846-855.

Figure Captions:

Figure 1. FTIR spectra obtained during the stepwise exposure of 0.5 (a), 2.5 (b) and 10 wt% (c) Pd/Al_2O_3 samples to CO_2 at 295 K. (The samples were annealed at 773 K for 2 h in vacuum prior to CO_2 exposure.)

Figure 2. Series of IR spectra obtained during the stepwise CO adsorption on annealed 0.5 (a), 2.5 (b) and 10 wt% (c) Pd/Al_2O_3 samples at 295 K. (The samples were annealed at 773 K for 2 h in vacuum prior to CO exposure.)

Figure 3. Series of IR spectra obtained during the stepwise CO adsorption on reduced 0.5 (a), 2.5 (b) and 10 wt% (c) Pd/Al_2O_3 samples at 295 K. (Prior to CO exposure the samples were reduced at 573 K in 0.4 Torr H_2 two times. After the second reduction step IR cell was evacuated and the samples were annealed at 773 K for 30 min, then cooled down to 295 K.)

Figure 4. FTIR spectra collected during the stepwise annealing of an oxidized (a) and reduced (b), CO saturated (at 100 K) 0.5 wt% Pd/Al_2O_3 sample to 300 K . (Prior to CO exposure the samples were oxidized at 573 K in 0.4 Torr O_2 two times. After the second oxidation the samples were cooled down to 295 K in O_2 and then the IR cell was evacuated. Reduction conditions were identical to that in Fig. 3. All the IR spectra were collected at 100 K sample temperature. Annealing was carried out in dynamic vacuum in 25 K increments.)

Figure 5. FTIR spectra collected during the annealing of an oxidized (a) and reduced (b), CO-saturated 2.5 wt% Pd/Al_2O_3 sample to 300 K. (Oxidation conditions were identical to that in Fig. 4. Reduction conditions were identical to that in Fig. 3.Annealing was carried out in dynamic vacuum in 25 K increments. All the IR spectra were collected at 100 K sample temperature.)

Figure 6. FTIR spectra collected during the stepwise annealing of the oxidized (a) and reduced (b), CO saturated 10 wt % Pd/Al_2O_3 sample to 300 K. (Oxidation conditions were identical to that in Fig. 4. Reduction conditions were identical to that in Fig. 3. Annealing was carried out in dynamic vacuum in 25 K increments. All the IR spectra were collected at 100 K sample temperature.)

Figure 1.

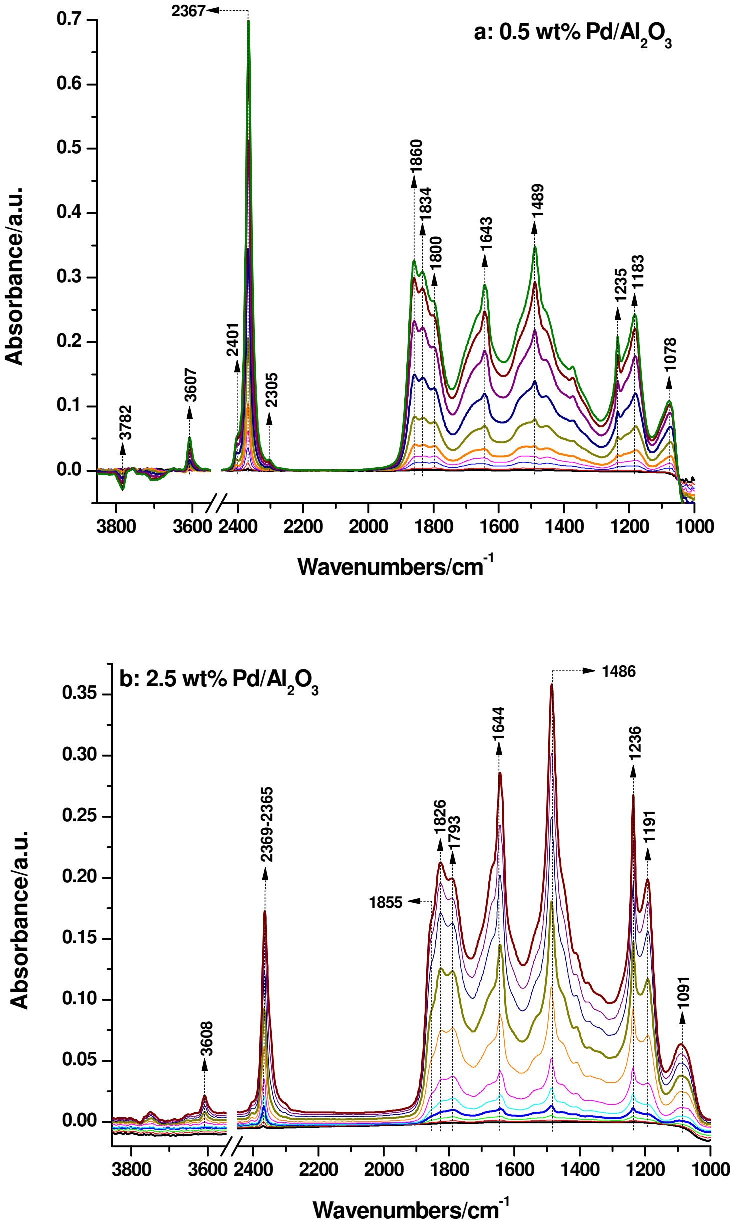
a: 0.5 wt% Pd/Al$_2$O$_3$
Absorbance/a.u.
0.7
0.6
0.5
0.4
0.3
0.2
0.1
0.0
2367
3782
3607
2401
2305
1860
1834
1800
1643
1489
1235
1183
1078
3800
3600
2400
2200
2000
1800
1600
1400
1200
1000
Wavenumbers/cm^{-1}
b: 2.5 wt% Pd/Al$_2$O$_3$
Absorbance/a.u.
0.35
0.30
0.25
0.20
0.15
0.10
0.05
0.00
1486
1644
1236
2369-2365
1826
1793
1191
1855
1091
3608
3800
3600
2400
2200
2000
1800
1600
1400
1200
1000
Wavenumbers/cm^{-1}

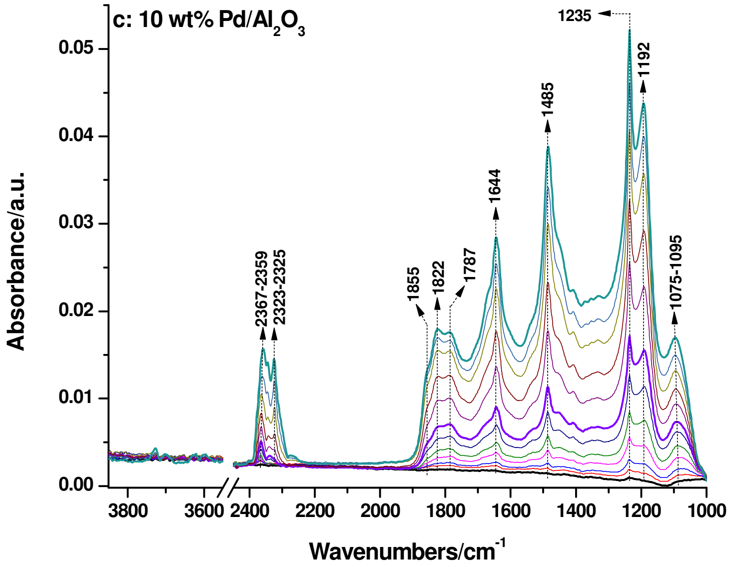
c: 10 wt% Pd/Al$_2$O$_3$
1235
1192
1485
1644
1855
1822
1787
2367-2359
2323-2325
1075-1095
Absorbance/a.u.
0.00
0.01
0.02
0.03
0.04
0.05
3800
3600
2400
2200
2000
1800
1600
1400
1200
1000
Wavenumbers/cm^{-1}

Figure 2.

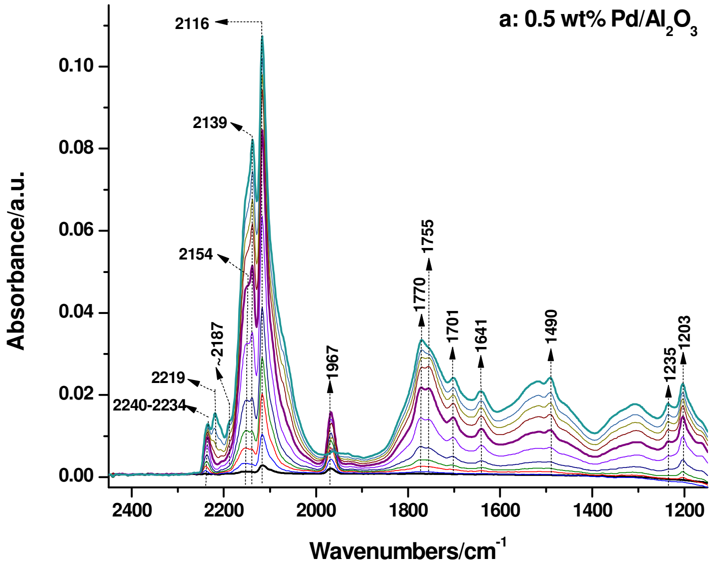
a: 0.5 wt% Pd/Al$_2$O$_3$
2116
2139
2154
2187
2219
2240-2234
1967
1770
1755
1701
1641
1490
1235
1203
Absorbance/a.u.
0.00
0.02
0.04
0.06
0.08
0.10
2400
2200
2000
1800
1600
1400
1200
Wavenumbers/cm^{-1}

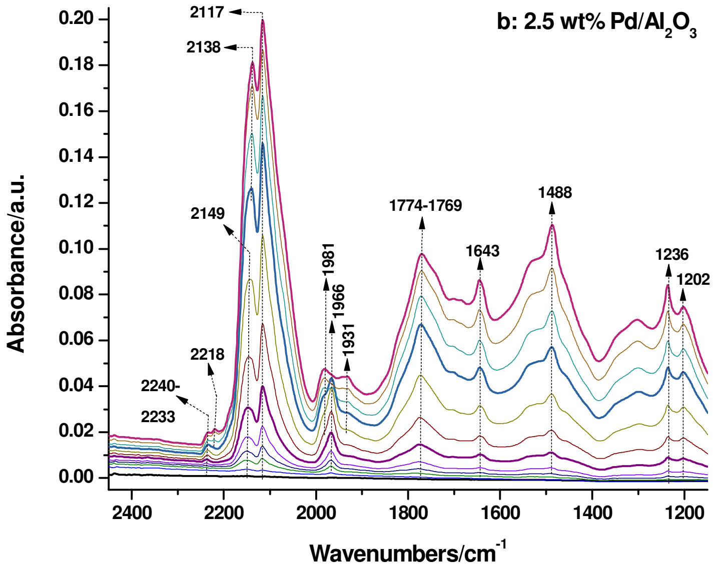
b: 2.5 wt% Pd/Al_2O_3
Absorbance/a.u.
Wavenumbers/cm^{-1}
0.00
0.02
0.04
0.06
0.08
0.10
0.12
0.14
0.16
0.18
0.20
2400
2200
2000
1800
1600
1400
1200
2117
2138
2149
2218
2240-
2233
1981
1966
1931
1774-1769
1643
1488
1236
1202

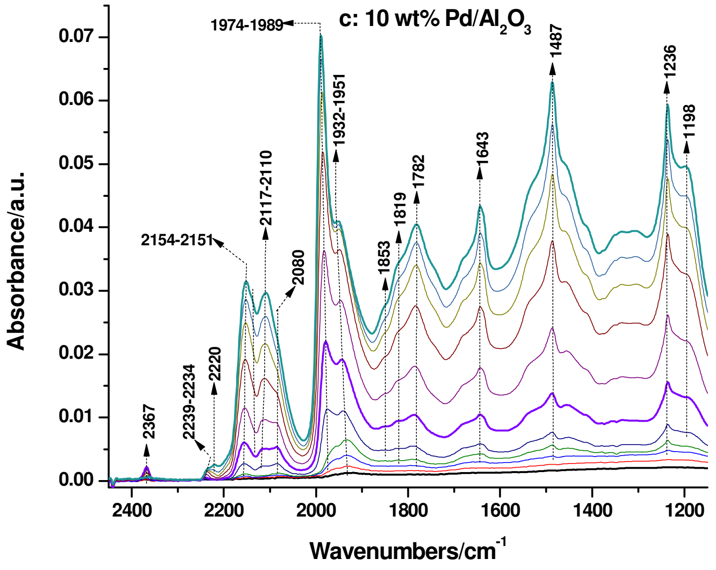
c: 10 wt% Pd/Al_2O_3
Absorbance/a.u.
Wavenumbers/cm^{-1}
0.00
0.01
0.02
0.03
0.04
0.05
0.06
0.07
2400
2200
2000
1800
1600
1400
1200
1974-1989
1932-1951
2117-2110
2154-2151
2080
2367
2239-2234
2220
1853
1819
1782
1643
1487
1236
1198

Figure 3.

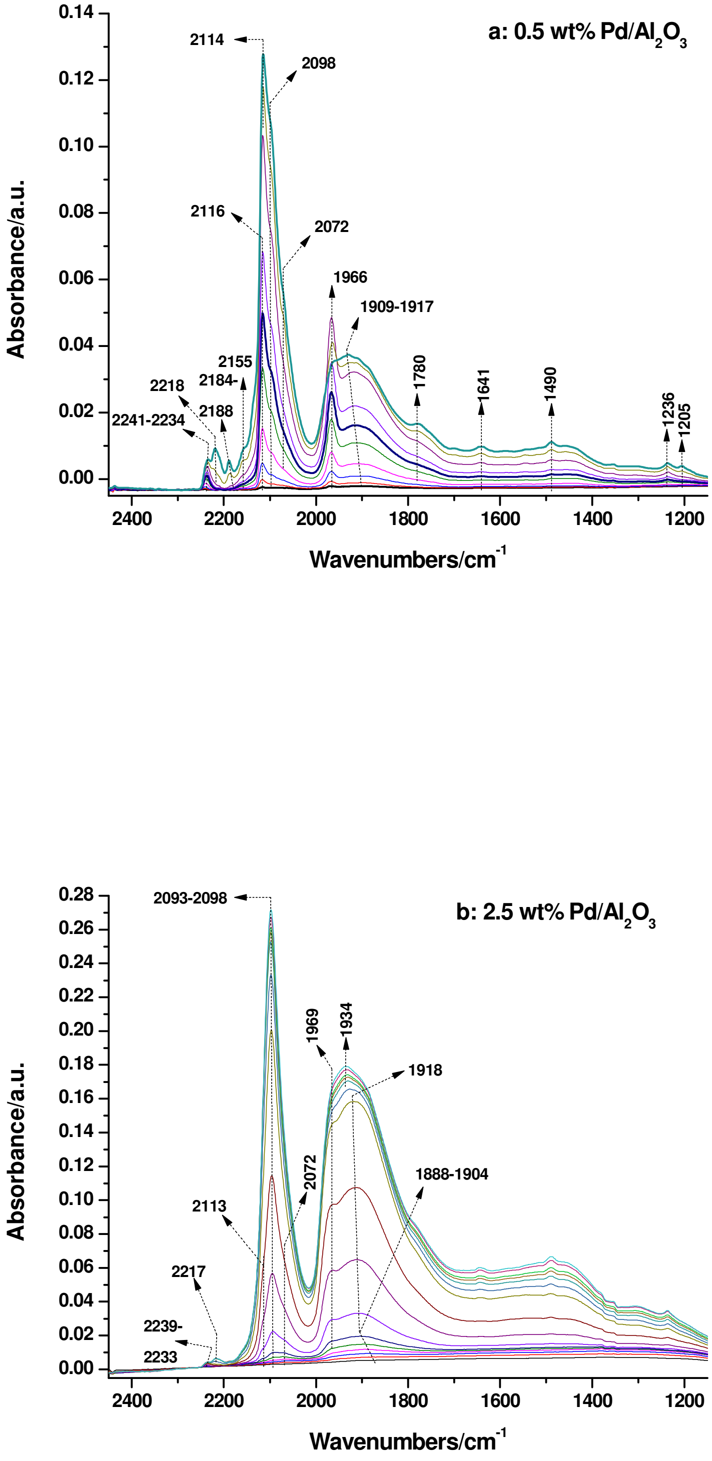
a: 0.5 wt% Pd/Al_2O_3
Absorbance/a.u.
0.14
0.12
0.10
0.08
0.06
0.04
0.02
0.00
2114
2098
2116
2072
1966
1909-1917
2155
2184-
2218
2188
2241-2234
1780
1641
1490
1236
1205
2400
2200
2000
1800
1600
1400
1200
Wavenumbers/cm^{-1}
b: 2.5 wt% Pd/Al_2O_3
Absorbance/a.u.
0.28
0.26
0.24
0.22
0.20
0.18
0.16
0.14
0.12
0.10
0.08
0.06
0.04
0.02
0.00
2093-2098
1969
1934
1918
2072
1888-1904
2113
2217
2239-
2233
2400
2200
2000
1800
1600
1400
1200
Wavenumbers/cm^{-1}

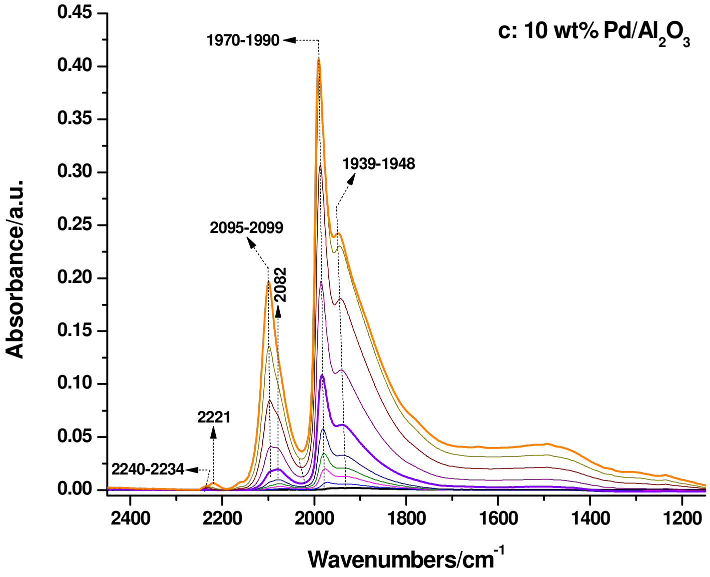
c: 10 wt% Pd/Al$_2$O$_3$
1970-1990
1939-1948
2095-2099
2082
2221
2240-2234
Absorbance/a.u.
0.45
0.40
0.35
0.30
0.25
0.20
0.15
0.10
0.05
0.00
2400
2200
2000
1800
1600
1400
1200
Wavenumbers/cm^{-1}

Figure 4.

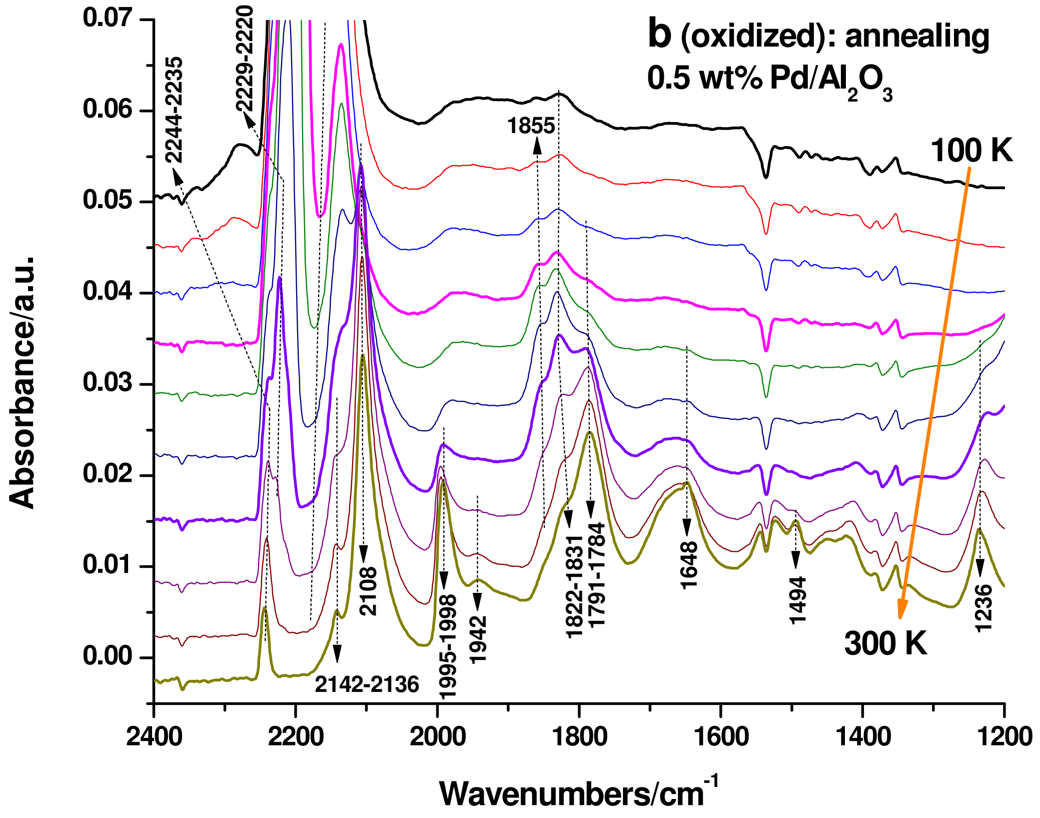
b (oxidized): annealing
0.5 wt% Pd/Al$_2$O$_3$
100 K
300 K
Absorbance/a.u.
Wavenumbers/cm^{-1}
0.07
0.06
0.05
0.04
0.03
0.02
0.01
0.00
2400
2200
2000
1800
1600
1400
1200
2244-2235
2229-2220
1855
2108
2142-2136
1995-1998
1942
1822-1831
1791-1784
1648
1494
1236

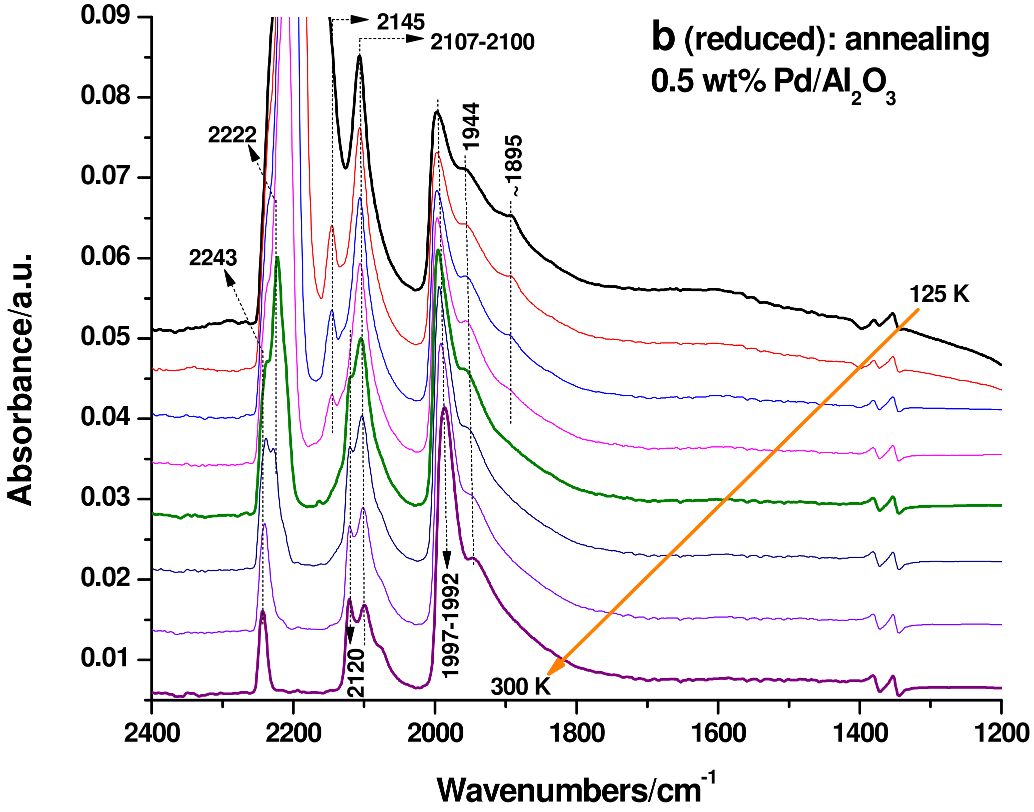
b (reduced): annealing
0.5 wt% Pd/Al$_2$O$_3$
Absorbance/a.u.
Wavenumbers/cm^{-1}
0.09
0.08
0.07
0.06
0.05
0.04
0.03
0.02
0.01
2400
2200
2000
1800
1600
1400
1200
2145
2107-2100
2222
2243
1944
~1895
125 K
300 K
2120
1997-1992

Figure 5.

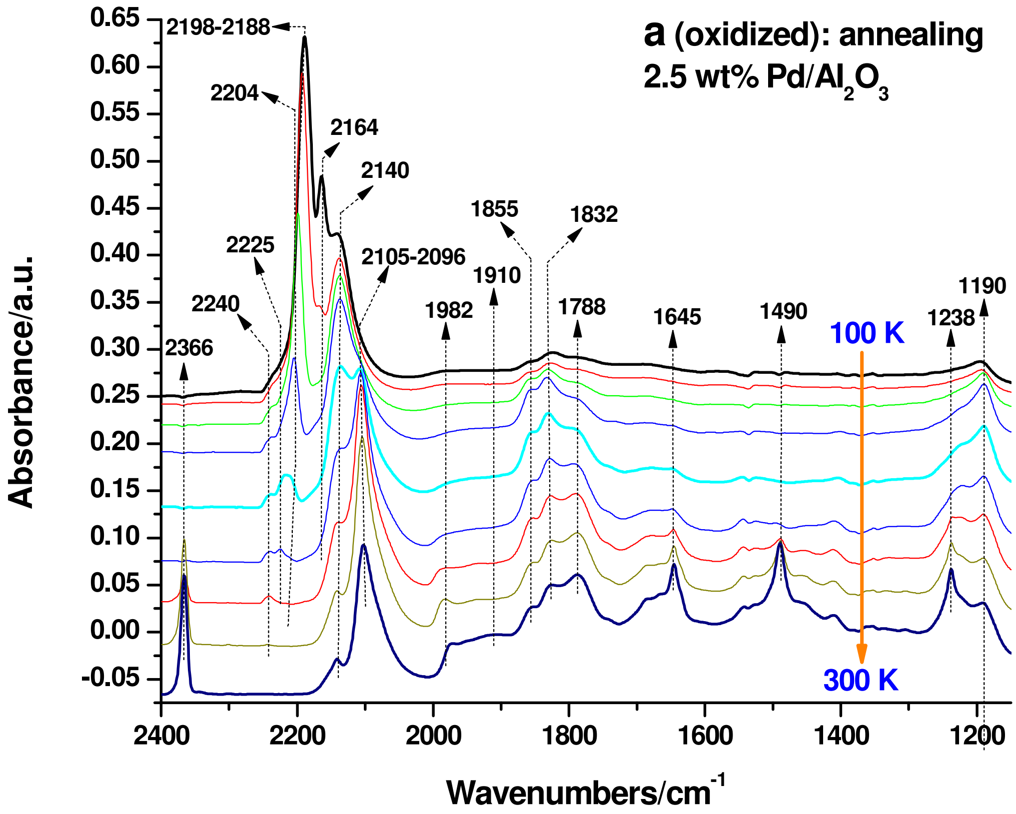
a (oxidized): annealing
2.5 wt% Pd/Al$_2$O$_3$
100 K
300 K
2198-2188
2204
2164
2140
2225
2240
2366
2105-2096
1982
1910
1855
1832
1788
1645
1490
1238
1190
Absorbance/a.u.
Wavenumbers/cm^{-1}
0.65
0.60
0.55
0.50
0.45
0.40
0.35
0.30
0.25
0.20
0.15
0.10
0.05
0.00
-0.05
2400
2200
2000
1800
1600
1400
1200

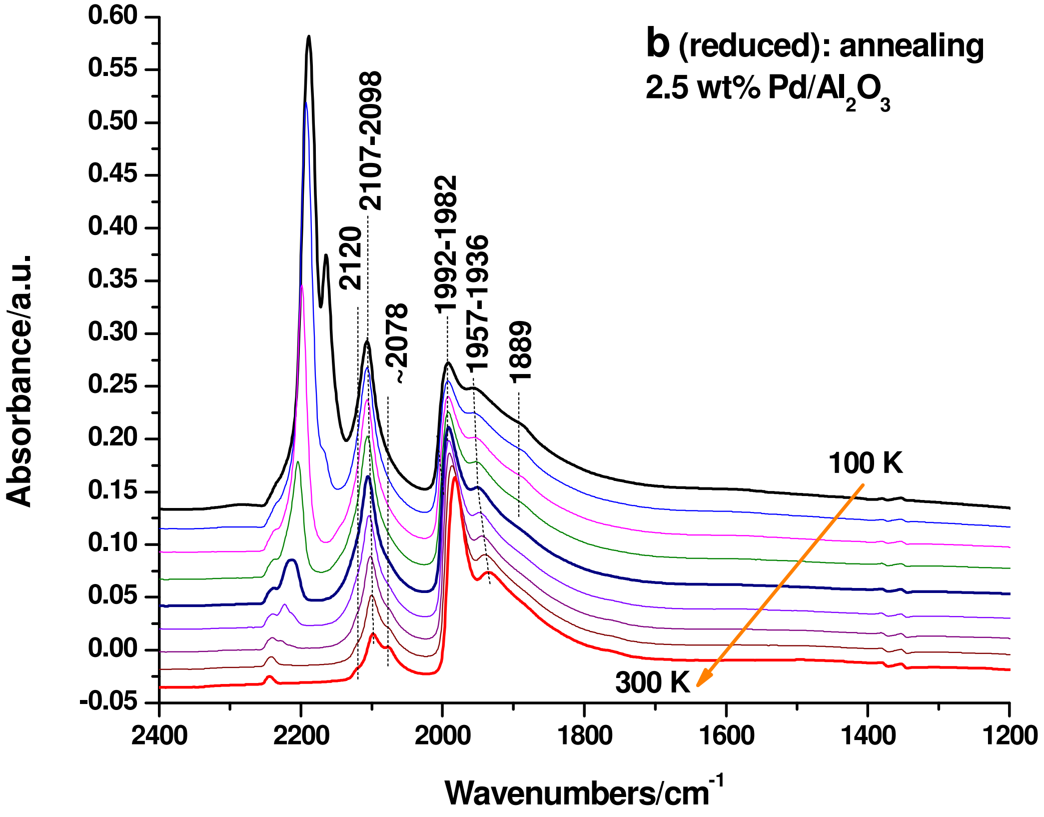
b (reduced): annealing
2.5 wt% Pd/Al_2O_3
Absorbance/a.u.
Wavenumbers/cm^{-1}
2120
2107-2098
~2078
1992-1982
1957-1936
1889
100 K
300 K
0.60
0.55
0.50
0.45
0.40
0.35
0.30
0.25
0.20
0.15
0.10
0.05
0.00
-0.05
2400
2200
2000
1800
1600
1400
1200

Figure 6.

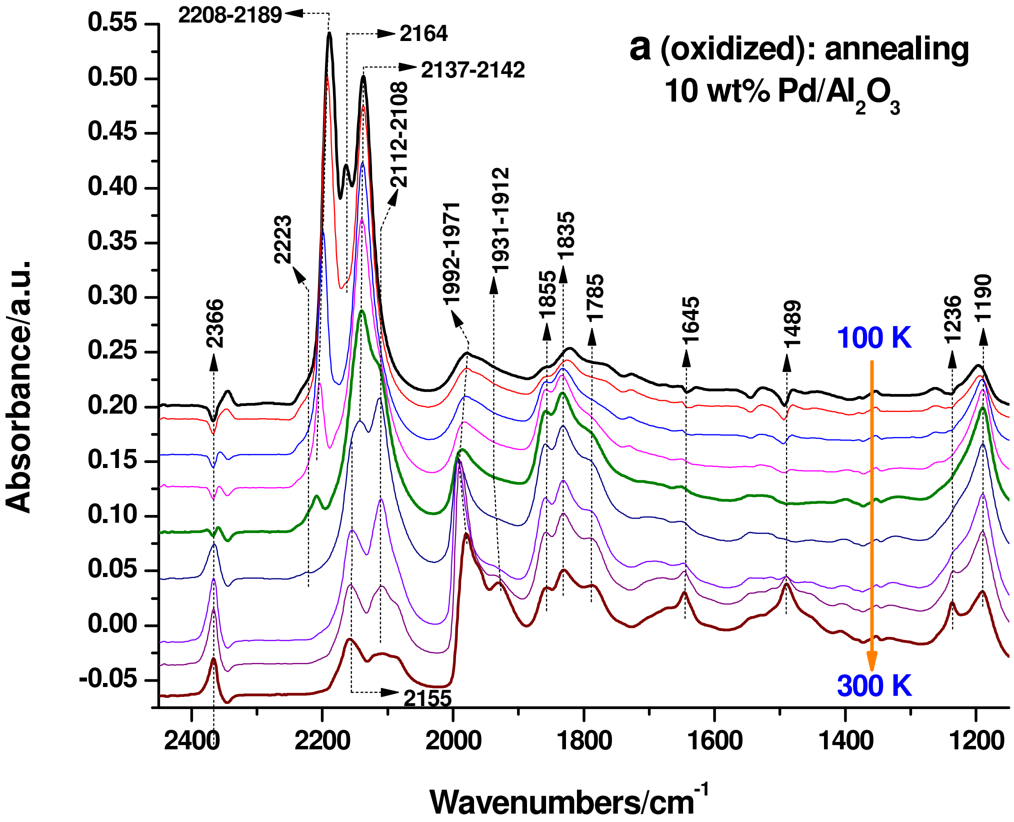
a (oxidized): annealing
10 wt% Pd/Al_2O_3
2208-2189
2164
2137-2142
2112-2108
2223
2366
1992-1971
1931-1912
1855
1835
1785
1645
1489
1236
1190
2155
100 K
300 K
Absorbance/a.u.
Wavenumbers/cm^{-1}
0.55
0.50
0.45
0.40
0.35
0.30
0.25
0.20
0.15
0.10
0.05
0.00
-0.05
2400
2200
2000
1800
1600
1400
1200

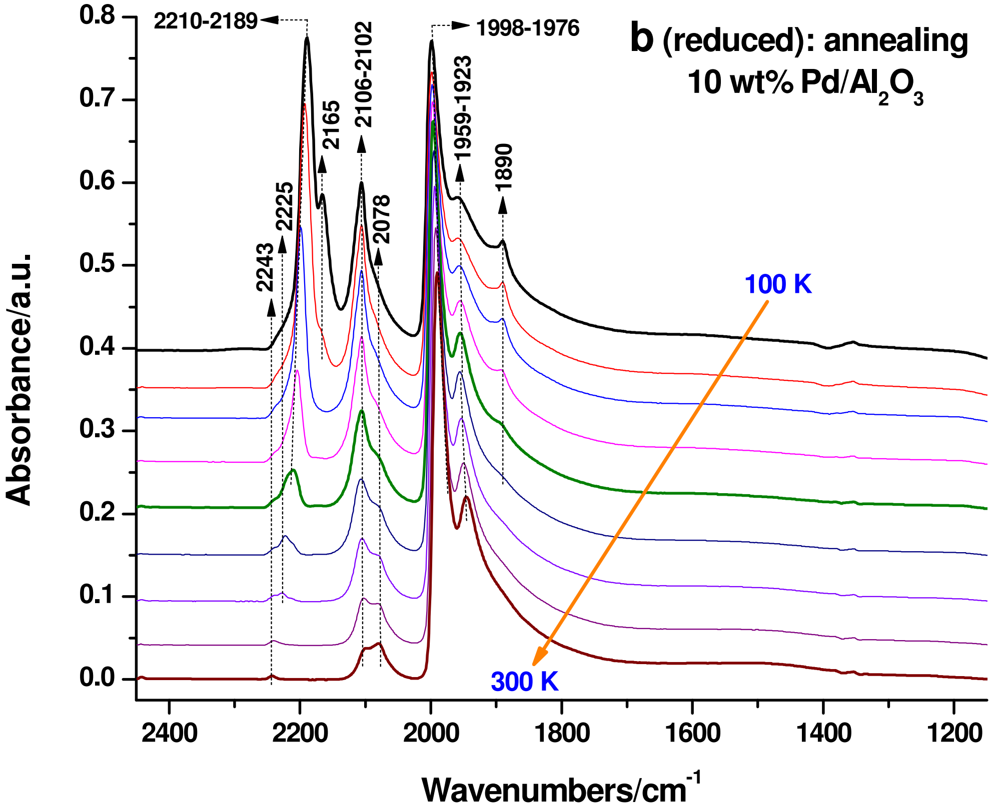
b (reduced): annealing
10 wt% Pd/Al_2O_3
2210-2189
2165
2106-2102
2078
2243
2225
1998-1976
1959-1923
1890
100 K
300 K
Absorbance/a.u.
0.0
0.1
0.2
0.3
0.4
0.5
0.6
0.7
0.8
2400
2200
2000
1800
1600
1400
1200
Wavenumbers/cm^{-1}

TOC.

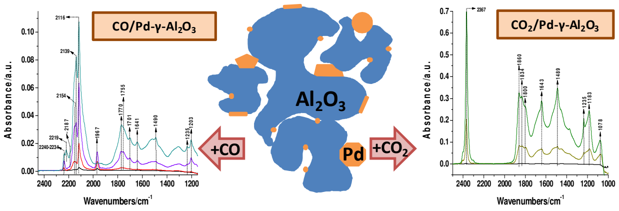
CO/Pd-γ-Al2O3
2116
2139
2154
2187
2219
2240-2234
1967
1770
1755
1701
1641
1490
1235
1203
Absorbance/a.u.
0.10
0.08
0.06
0.04
0.02
0.00
2400
2200
2000
1800
1600
1400
1200
Wavenumbers/cm-1
+CO
Al2O3
Pd
+CO2
CO2/Pd-γ-Al2O3
2367
1860
1834
1800
1643
1489
1235
1183
1078
0.7
0.6
0.5
0.4
0.3
0.2
0.1
0.0
1000